



## **Algicidal activity and DNA binding affinity of silver nanoparticle- biofabricated by green alga, *Rhizoclonium riparium***

Piya Roychoudhury<sup>1</sup>, Rahul Bose<sup>2</sup> and Ruma Pal<sup>2</sup>

<sup>1</sup>Department of Botany, Karnatak Arts, Science and Commerce College, Bidar-585401, Karnataka, Email: [piyaroychoudhury2@gmail.com](mailto:piyaroychoudhury2@gmail.com);

<sup>2</sup>Department of Botany, University of Calcutta, 35, Ballygunge Circular Road, Kolkata- 700 019, India

---

### **Abstract**

Green alga, *Rhizoclonium riparium* was treated with silver nitrate solution (9 mM) for synthesis of biocompatible silver nanoparticle (SNP). After 72 h of reaction, the filaments of *Rhizoclonium* turned dark brown in color and initially synthesis of SNP was confirmed by observing absorption maxima at 415 nm in Uv-vis spectroscopy. The crystallographic nature and purity of particles were analysed by X-ray powder diffraction (XRD) and Energy dispersive X-ray spectroscopy (EDAX) respectively. Fourier transform infrared spectroscopy (FTIR) confirmed the presence of C-H, N-H, C-C, C-O functional groups on SNP surface. Recorded surface charge of SNP was – 41.4 mV. Transmission Electron Microscopy (TEM) revealed that SNPs were spherical in nature with ~2-40 nm in size. The binding affinity between DNA and SNP was tested by agarose gel electrophoresis. TEM micrographs of SNP-DNA showed the particles arrangement in a series adjoining with each other. Algicidal activity of SNP against unicellular alga, *Chlorococcum infusionum* was confirmed by agar well diffusion method. Upregulation of stress enzymes such as catalase, super oxide dismutase and ascorbate peroxidase together with carotenoid content were recorded against Ag<sup>+</sup> stress. Extracted carotenoids, proteins and chloroplasts from *Rhizoclonium* also showed high efficiency in reduction of Ag<sup>+</sup> ions and subsequent production of SNP.

**Keywords:** Alga; Silver nanoparticle; Nanosilver-DNA; Algicide; Microscopy, Spectroscopy

---

### **Introduction**

Silver particle is a well recognized antimicrobial agent (Lara et al. 2010). It has been already reported that SNP is nontoxic to human but showed its effectiveness against microbes at very low concentration (Jeong et al. 2005). The antimicrobial property of SNP has been exploited in different products such as textiles, food storage containers, home appliances and especially in medical devices (Marambio-Jones et al. 2010) and in pesticide filter (Pradeep and Anshup, 2009). SNP is also used in tropical ointments to prevent infection against burn and open wounds (Ip et al. 2006). The antibacterial activity of SNP and their mechanism against bacteria has been fully elucidated (Lara et al. 2010). SNPs directly interact with the cell surface of various bacteria and damaged cell membranes making it more permeable (Sondi and Salopek-Sondi. 2004). Nanosilver has been reportedly used in various medical applications viz. imaging, hyperthermia of tumors and drug delivery (Daniel et al. 2004; Lee et al. 2008). However, the algicidal activity of biogenic nanoparticle has not been reported yet.

The DNA-SNP conjugates have already been exploited as plasmonic biosensors (Huang et al. 2008) and molecular electronics. SNP can interact with cytosine of DNA because in cytosine, presence of lone pair exocyclic nitrogen takes part in binding with SNP (Liu and Huang, 2012). Till date, several exciting methods have been reported for preparation of DNA–SNP conjugates (Liu and Huang, 2012); however, these methods pose serious challenge for researchers. This challenge arises from the chemical degradation of the SNPs during the long incubation period and high silver oxidation reactivity. Thus, to extend the application of DNA–SNP conjugates in the analytical field, a well accepted method for preparing DNA–SNP conjugates is highly desired.

Synthesis of SNP by using different bioreagents like bacteria (Gurunathan et al. 2009; Samadi et al. 2009; Pugazhenthiran et al. 2009; Ganes Babu and Gunasekaran 2009; Nanda and Saravanan 2009; Sintubin et al. 2009; Kalishwaralal et al. 2010) cyanobacteria (Lengke et al. 2007, Roychoudhury and Pal, 2014), fungi (Ahmad et al. 2003; Shaligram et al. 2009; Mukherjee et al. 2001; Ingle et al. 2008; Verma et al. 2010) and higher plants (Shankar et al. 2004; Huang et al. 2007) are well documented. Few reports are there which have identified the reducing capability of cellular components during SNP production such as fucoxanthin extracted from diatom *Amphora* (Jena et al. 2014); protein from fungus *Rhizopus* (Das et al. 2012) are able to synthesize SNP.

In this study, we synthesized SNP using fractionated cellular components (Carotenoids, Protein and Chloroplasts) of green alga, *Rhizoclonium* with comprehensive characterizations using UV-vis spectroscopy, TEM, SEM, DLS, Zeta, XRD and EDAX studies. The algicidal effect and interaction with DNA of SNP was also observed.

## Materials and Methods

### *Biogenesis of SNP using green alga R. riparium*

The eukaryotic alga, *R. riparium* was collected from Calcutta University culture collection (CUH/AL/ MW48) and it was maintained in Bold Basal Media at 20°C under 20–30  $\mu\text{mol photons m}^{-2} \text{s}^{-1}$  from 'cool' fluorescent lights with 16: 8 hrs light and dark cycle. Healthy filaments (500 mg) of *R. riparium* were exposed to 100 ml 9 mM aqueous  $\text{Ag}^+$  ( $\text{AgNO}_3$ ; MW 169.87; SRL, Mumbai, India) solution at pH 4 (as pH 4 showed best results). The experimental set was kept in dark at room temperature for 7 days. The extraction and purification of SNP from nanoparticle loaded filaments was performed according to the protocol of Roychoudhury et al. (2016). The extracted suspension was subsequently utilized for characterizations of SNP.

The maximum absorbance of synthesized SNP was analysed with a Thermo Evolution 300 UV-visible spectrophotometer (Waltham, USA) in wavelength range of 300-1100 nm. The crystallographic nature of SNP was confirmed by XRD study. The SNP loaded biomass was air-dried, grinded into powder using mortar and pestle and the XRD spectra were studied with a Panalytical PW 3040/60, DY 2501 X-ray diffractometer (Amsterdam, Netherland) from 5° to 100° 2 $\theta$  angles using Cu K $\alpha$  radiation operated at 40 kV and 30 mA. The purity of SNP suspension was confirmed by EDAX study. A drop of extracted brown suspension was dried overnight on a carbon coated copper grid and EDAX signals were measured by JEOL JEM 2100 HR-EDAX (JEOL, Tokyo, Japan). The FTIR spectra of the synthesized SNP were recorded with Jasco FTIR-6300 (USA) in the range between 4000 and 400  $\text{cm}^{-1}$ . The DLS and Zeta study was performed using a particle analyzer (Nano ZS, Malvern). A drop of SNP extract was dried on a carbon coated copper grid and the size-shape analysis was carried out by JEOL JEM 2100 HR-TEM (JEOL, Tokyo, Japan). The surface changes in silver loaded filaments were observed by scanning electron microscope (SEM). Some filaments were taken on glass cover slip and vacuum dried. The appropriately dried sample was gold coated and surface of the filament was scanned using Carl Zeiss EVO 18 SEM (Jena, Germany). The change of fluorescent property of silver loaded filaments was observed by Axioscope A1 Zeiss fluorescence microscope (excitation: 450-490 nm and emission: 515 nm).

### *DNA and SNP interaction*

First, silver particles were lyophilized to measure the concentration of SNP per mL of supernatant. Then the lyophilized SNP was properly washed with deionized water and resuspended within water. Five different concentrations of SNP like 0.1, 0.2, 0.3, 0.4 and 0.5  $\text{mg ml}^{-1}$  were selected to confirm the SNP-DNA binding affinity. Algal DNA was extracted from green alga, *Chlorococcum infusionum* (AL/CCCU/ FW-18) following the methods of Doyle and Doyle (1990). The extracted algal DNA (4  $\mu\text{l}$ ) and synthesized SNP particles (4  $\mu\text{l}$ ) were mixed and incubated for 30 min. After incubation the mixtures were subjected to agarose gel electrophoresis with 0.8% gel concentration. The observed DNA bands were documented with Vilber Quantum ST5 gel doc, Australia. The binding pattern of the particles with DNA was also observed under TEM after incubation. The highest concentration of particles (0.5  $\text{mg ml}^{-1}$ ) was selected for TEM study since it showed the best result in agarose gel electrophoresis.

### *Algicidal activity of SNP*

Algicidal activity of biosynthesized SNP was determined by agar well diffusion method against unicellular green alga, *Chlorococcum infusionum* (AL/CCCU/ FW-18). The algal strain was procured from Calcutta University culture collection (Kolkata, West Bengal, India). Initially, the alga was grown in Bold Basal Media at 25°C in 16:8 hour light: dark cycle under cool fluorescent light having intensity 20-30  $\mu\text{mol m}^{-2}\text{s}^{-1}$ . After 10 days of culturing, inoculum of *Chlorococcum infusionum* was uniformly spread in 1.5% agar BBM agar plate. In agar plate two cavities were prepared by a well-cutter and one cavity was filled with 50  $\mu\text{L}$  of SNP suspension (0.5  $\text{mg mL}^{-1}$ ) and another one was filled with sodium citrate as SNPs were suspended in citrate solution. The agar plate was incubated at 25°C for 10 days and diameter of the clear zone was measured. The cells of *Chlorococcum* were exposed directly in SNP for 10 days and morphological changes were observed.

### *Study of biochemical parameters in silver exposed Rhizoconium*

Associated biochemical changes in *R. riparium* during interaction with lethal (9 mM) and sublethal (1 mM) doses of  $\text{Ag}^+$  (pH 4) solution were studied at different time intervals (10 min, 30 min, 1 h, 3 h and 24 h). All the experiments were done in triplicates. A control set was maintained for each experiment. Different biochemical parameters like chlorophyll and carotenoid, carbohydrate and protein contents were measured following standard methods of Arnon (1949); Hodge et al. (1962); Lowry et al. (1951) respectively. Various stress enzyme's viz. superoxide dismutase (SOD), ascorbate peroxidase (APX) and catalase (CAT) activity were also estimated following methods of Beauchamp and Fridovich (1971); Sadashivam and Manickam (1996) and Nakano and Asada (1981) respectively.

### *Identification of reducing cellular components in eukaryotic algae*

The bioactive cellular components like carotenoids, proteins and chloroplasts were extracted from healthy biomass of *R. riparium*. Carotenoids, total protein and chloroplasts were extracted following standard methods of

Arnon (1949); Lowrey et al. (1951) and Kunst et al. (1988) respectively. Carotenoids (~0.9 mg), proteins (~12.5 mg), chloroplasts (~ 2 mg) were exposed to 100 ml 9 mM aqueous  $\text{Ag}^+$  ( $\text{AgNO}_3$ ; MW 169.87; SRL, Mumbai, India) solution at pH 4 separately under ambient condition. The experimental sets of proteins were maintained at 4°C. The SNP was extracted from chloroplast by following the nanoparticle extraction procedure mentioned in Roychoudhury et al. (2016). The absorption spectra, size and shape of the synthesized SNP was investigated by UV-Vis spectroscopy and Transmission Electron Microscope respectively.

## Results

Brownish color appeared in green filaments of *R. riparium* after 3 h of reaction with  $\text{Ag}^+$  ions (Fig 1). All filaments turned dark brown in color after 72 h of exposure in silver solution. SEM study clearly provided the difference of surface topography between control and silver-treated filaments of *R. riparium* (Fig 1g&h). The surface of treated filaments was covered by silver nanosphere in contrast to smooth surface topography of control filaments. In fluorescent microphotographs (Fig 1e&f) silver treated filaments emitted green fluorescence contrasting the red fluorescent property of control filaments. In Uv-vis spectroscopy, SNP showed maximum absorbance at 415 nm (Fig 2a). In XRD experiment,  $2\theta$  values observed at 38.2°, 44.5°, 64.8° and 77.8° that can be indexed at (111), (200), (220) and (311) lattice planes (Fig 2b). EDAX study showed a strong signal of silver (Fig 2c). In FTIR study distinct peaks observed at 3400, 2937, 2363, 2352, 1671, 1076, and 670  $\text{cm}^{-1}$  (Fig 2d). The hydrodynamic diameter of SNP was recorded as 58.71 nm. The surface charge of SNP was – 41.4 mV, confirmed by zeta potential study.

**Fig 1** Whole biomass of *R. riparium* turned brown (b) in color after treatment with silver nitrate contrasting the green color of control biomass of (a). Control (c) and Ag treated (d) filament of *Rhizoclonium*. Fluorescent microscopic image of control (e) and Ag treated (f) filament of *R. riparium*. SEM images showing the surface topography of control (g) and SNP loaded filament (h). Red arrows are showing SNP deposition on the algal surface.

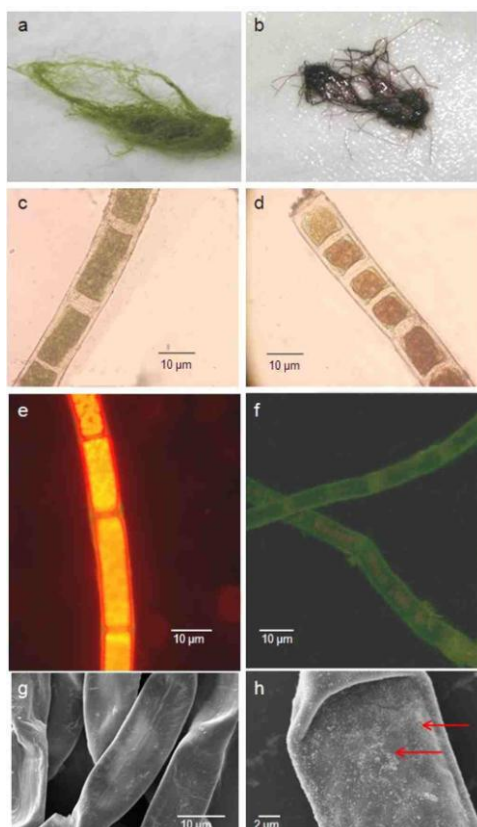


**Fig 2** Uv-vis spectrum of extracted nanosuspension showing the maximum absorbance at 415nm (a). XRD patterns of biosynthesized silver nanoparticles (b). EDAX signal confirms the presence of silver in biosynthesized brown colored nanosuspension(c). FTIR spectrum of synthesized particles confirms the presence of different functional groups on the particle surface.

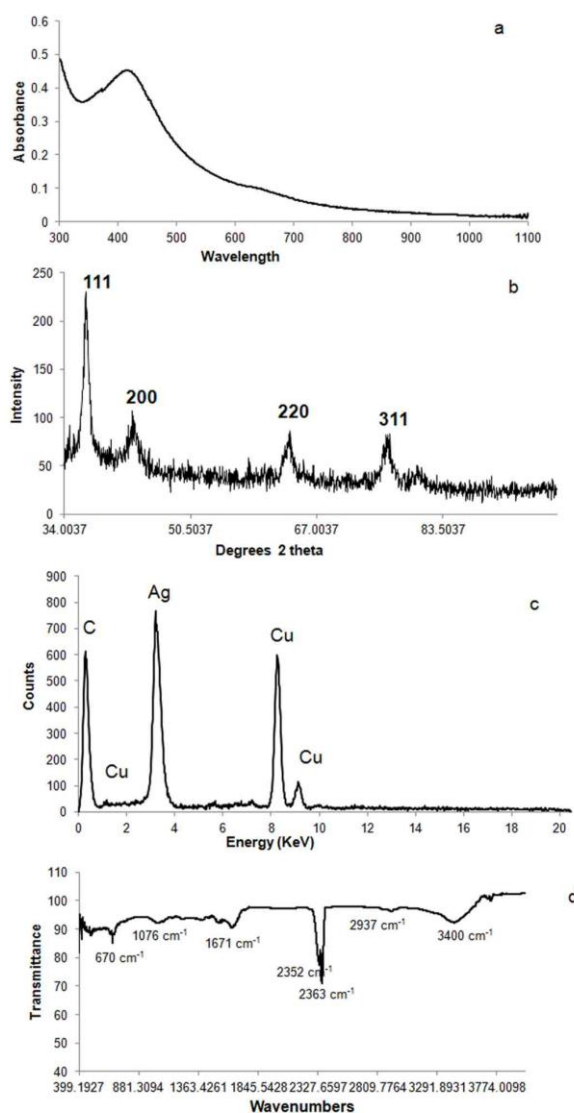


**Fig 2** Uv-vis spectrum of extracted nanosuspension showing the maximum absorbance at 415nm (a). XRD patterns of biosynthesized silver nanoparticles (b). EDAX signal confirms the presence of silver in biosynthesized brown colored nanosuspension(c). FTIR spectrum of synthesized particles confirms the presence of different functional groups on the particle surface.

From TEM study it was confirmed that synthesized SNPs were spherical in nature with ~2-40 nm in size (Fig 3a&b). Agarose gel electrophoresis of DNA-SNP revealed that the band intensity of DNA decreased with increasing SNP concentration (Fig 3c). No band was observed in lane 2 (SNP concentration  $0.5\text{mg ml}^{-1}$ ). TEM micrographs of SNP-DNA also confirmed the binding affinity of SNP with DNA as the particles were arranged in a series adjoining with each other (Fig 3d&e).

**Fig 3** TEM images showing the synthesized SNP by *Rhizoclonium* are spherical in nature (a-b). Agarose gel electrophoresis of DNA mixed with SNP showing the decrease of band thickness with increase of particle concentration (c)-Lane 1 showing the intensity of control DNA band extracted from green alga, *Chlorococcum*. Six Different concentrations of the synthesized particles like 0.1 (Lane 3), 0.2 (Lane 4), 0.3 (Lane 5), 0.4 (lane 6) and  $0.5\text{ mg ml}^{-1}$  (Lane 2) were used in six different lanes and no DNA band was observed in lane 2 where the maximum particle concentration ( $0.5\text{ mg ml}^{-1}$ ) was used. TEM study of DNA-SNP showing the particles are arranged in a series adjoining with each other after interaction with DNA [Scale bar: 20 nm] (d-e).

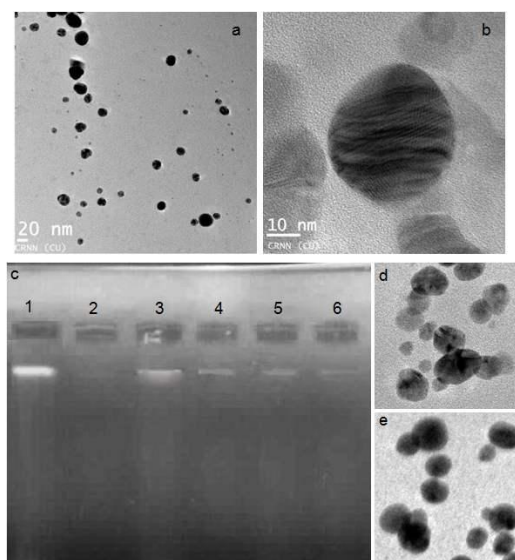


**Fig 3** TEM images showing the synthesized SNP by *Rhizoclonium* are spherical in nature (a-b). Agarose gel electrophoresis of DNA mixed with SNP showing the decrease of band thickness with increase of particle concentration (c)-Lane 1 showing the intensity of control DNA band extracted from green alga, *Chlorococcum*. Six Different concentrations of the synthesized particles like 0.1 (Lane 3), 0.2 (Lane 4), 0.3 (Lane 5), 0.4 (lane 6) and 0.5 mg ml<sup>-1</sup> (Lane 2) were used in six different lanes and no DNA band was observed in lane 2 where the maximum particle concentration (0.5 mg ml<sup>-1</sup>) was used. TEM study of DNA-SNP showing the particles are arranged in a series adjoining with each other after interaction with DNA [Scale bar: 20 nm] (d-e).

The SNP showed algicidal activity against eukaryotic alga, *Chlorococcum infusionum*. The maximum zone of inhibition (7 mm) was found at 0.5mg ml<sup>-1</sup> concentration. Sodium citrate showed no effect against algae (Fig 4d). The deposition of SNP in cell wall of *Chlorococcum* was observed after 72 h of exposure in SNP suspension. After 10 days of exposure maximum portion of cell wall was turned brown in color (Fig 4a-c).

**Fig 4** algicidal activity of SNP against *Chlorococcum infusionum*. (a) Control cell of *C. infusionum*. SNP treated cell after 24 h (b) and after 72 h (c); Red arrows indicating the appearance of brown color in SNP treated cells. (d) Agar plate showing the inhibition zone.

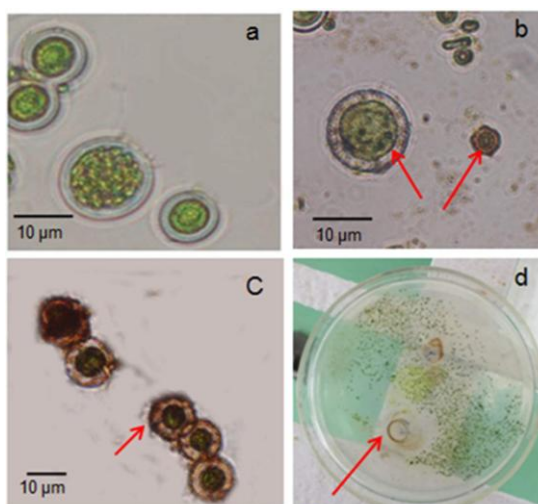


**Fig 4** algicidal activity of SNP against *Chlorococcum infusionum*. (a) Control cell of *C. infusionum*. SNP treated cell after 24 h (b) and after 72 h (c); Red arrows indicating the appearance of brown color in SNP treated cells. (d) Agar plate showing the inhibition zone

In *R. riparium* protein content increased at sublethal (1 mM) dose of silver, whereas in lethal dose (9mM, nanoparticle forming dose) the protein content initially increased (2.6 times) upto 30 min of reaction followed by a decrease. Slight increase of carbohydrate content (1.5 fold) was recorded in metal exposed biomass compared to the control biomass. A drastic decrease of chlorophyll content in both lethal and sublethal doses was recorded. Carotenoid content increased steadily up to 3 h (1.6 fold increase than control) followed by a decrease. In lethal dose of silver (9 mM) APX activity was upregulated (5.5 times) within 30 mins of reaction,

whereas in sublethal dose it increased (2.6 times) upto 24 h of reaction. CAT activity increased in sublethal (2.6 fold) and lethal (8.26 fold) doses related to reaction time. SOD activity also increased after treatment with lethal (2.5 fold) and sublethal (1.7 fold) doses of metals (Table 1).

Extracted carotenoids, proteins and chloroplasts from green alga, *R. riparium* showed their high efficiency in reduction of Ag<sup>+</sup> ions and subsequent production of SNP. The spectral analysis of synthesized SNP by extracted carotenoids, proteins and chloroplasts showed maximum absorbance at 422nm, 428 and 431 nm respectively (Fig 5). TEM study revealed that the particles synthesized by carotenoid extracts are mixture of different shapes like spherical, triangular, oval, hexagonal, rod and irregular etc. with variable size range (15-60 nm). Whereas the particles synthesized by extracted proteins and chloroplasts are all spherical in nature. The SNP produced by protein extract are 2-15 nm in diameters. The size range of SNP synthesized by chloroplast extract is 5-45 nm (Fig 6).

## Discussion

Brown color appeared in *Rhizoclonium* filament due to the reduction of Ag<sup>+</sup> ions at intracellular level and subsequent formation and deposition of SNP within algal filaments (Roychoudhury and Pal, 2014). Number of cells increased within a filament due to high rate of cell division in silver stress (Fig 1c&d). High rate of cell division is a common stress response which was also mentioned by Parial et al. (2015) in gold treated *Rhizoclonium*. Silver treated filaments emitted green fluorescence due to increase of carotenoid content in metal stress as also reported by Kleinegriss et al. (2010) in *Dunaliella*. The silver-treated filament stored carotenoids in lipid globules (secondary carotenogenesis) and increased the green fluorescence with exposure time.

**Table 1 Showing changes in biochemical parameters of control and silver-exposed biomass with time [maximum values (mean±SE) in silver exposed biomass are indicated as bold and italic]**

Parameters	Control/ treated	Time				
		10 min	30 min	1 h	3 h	24 h
Protein (mg g <sup>-1</sup> )	Control	22.644±0.11	23.528±0.17	24.072±0.23	24.684±0.11	25.296±0.11
	1 mM Ag treated	30.124±0.29	31.076±0.17	36.992±0.18	39.236±0.30	43.248±0.31
	9 mM Ag Treated	51.884±0.49	<b>60.044±0.47</b>	48.28±0.24	32.436±0.42	24.956±0.29
Chlorophyll (mg g <sup>-1</sup> )	Control	2.95±0.09	3.05±0.09	3.21±0.06	3.37±0.11	3.53±0.058
	1 mM Ag treated	2.79±0.067	2.70±0.083	2.48±0.094	2.11±0.058	1.92±0.094
	9 mM Ag Treated	<b>2.25±0.08</b>	2±0.09	1.65±0.16	1.16±0.08	1.02±0.02
Carotenoids (mg g <sup>-1</sup> )	Control	1.748±0.002	1.758±0.003	1.784±0.005	1.796±0.002	1.86±0.06
	1 mM Ag treated	2.12±0.005	2.27±0.009	2.34±0.002	2.38±0.007	2.4±0.008
	9 mM Ag Treated	1.79±0.002	2.596±0.007	2.84±0.014	<b>2.976±0.003</b>	2.80±0.002
Carbohydrate (mg g <sup>-1</sup> )	Control	24.97±0.082	24.95±0.088	28.12±0.64	29.316±0.26	30.192±0.44
	1 mM Ag treated	30.48±0.14	32.86±0.44	35.07±0.003	35.96±0.51	39.07±0.49
	9 mM Ag treated	31.96±0.25	39.81±0.39	42.62±0.001	<b>44.25±0.29</b>	30.48±0.14
APX (mM min <sup>-1</sup> mg protein <sup>-1</sup> )	Control	0.099±0.01	0.116±0.005	0.123±0.005	0.135±0.004	0.146±0.006
	1 mM Ag treated	0.181±0.004	0.225±0.003	0.241±0.006	0.291±0.005	0.319±0.003
	9 mM Ag treated	0.426±0.007	<b>0.674±0.008</b>	0.399±0.004	0.381±0.003	0.309±0.004
CAT (mM min <sup>-1</sup> mg protein <sup>-1</sup> )	Control	0.149±0.037	0.179±0.036	0.175±0.035	0.239±0.034	0.267±0.033
	1 mM Ag treated	0.374±0.047	0.453±0.045	0.495±0.038	0.503±0.036	0.553±0.032
	9 mM Ag treated	1.141±0.081	<b>1.47±0.12</b>	1.401±0.087	1.304±0.13	0.677±0.16
IC <sub>50</sub> of SOD (mg protein <sup>-1</sup> )	Control	0.068±0.001	0.0712±0.21	0.073±0.033	0.0751±0.11	0.0765±0.001
	1 mM Ag treated	0.0911±0.002	0.0941±0.003	0.112±0.002	0.119±0.001	0.131±0.005
	9 mM Ag treated	0.158±0.003	<b>0.182±0.14</b>	0.146±0.005	0.098±0.27	0.075±0.01

Nanosilver exhibits brown color due to localized surface plasmon resonance (LSPR). The absorption maxima within 415-420 nm indicated the presence of spherical shaped SNP (Lu et al. 2006; Shankar et al. 2004). In our study also, the absorption peak appeared at 415 nm indicating possible synthesis of spherical SNP and it was confirmed by TEM study. The extracted nanosuspension showed the absorbance maxima at the same position

upto one month, and no significant peak shift was observed. This character confirms the stability of synthesized SNP. The stability of SNP was also confirmed by zeta potential study.

The four intense peaks recorded in XRD study followed the Bragg's rule and confirmed the fcc crystallographic nature of synthesized SNP (MubarakAli et al. 2011). EDAX study showed only the signal of silver which confirmed the purity of SNP, not contaminated by other particles (Fig 2c). FTIR spectrum revealed the presence of different functional groups on the surface of SNP. The IR peak at 3400 indicated strong stretching vibrations of N- H functional group (Faramarzi and Forootanfar, 2011). The peaks at 2937, 1076 and 670  $\text{cm}^{-1}$  were assigned to C-H vibrations (Gole et al. 2001; Rajasekharreddy et al. 2010) and the IR band at 1671  $\text{cm}^{-1}$  indicated C-O stretching. The distinct peaks recorded at 2363 and 2352  $\text{cm}^{-1}$  were mainly for C-C stretching (Gajbhiye et al. 2009).

The hydrodynamic diameter of NPs includes the inorganic core along with coating material and the solvent layer attached to the particle as it moves under the influence of Brownian motion. For this reason hydrodynamic diameter measured by DLS study was greater than the diameter observed in TEM study. In suspension when the particles will be highly negatively or positively charged, the degree of repulsion between adjacent particles will be more. High repulsion resists aggregation and precipitation. Here synthesized SNPs by *R. riparium* showed high stability with negative zeta potential value (Fen et al. 2013). From TEM study it was confirmed that synthesized SNPs were variable in size (Fig 3a&b). Size variation is very common in biogenic synthesis due to presence of more than one reducing agent.

**Fig 5** Uv-vis spectra of the SNP synthesized by extracted protein, chloroplast and carotenoids of *Rhizoclonium*.

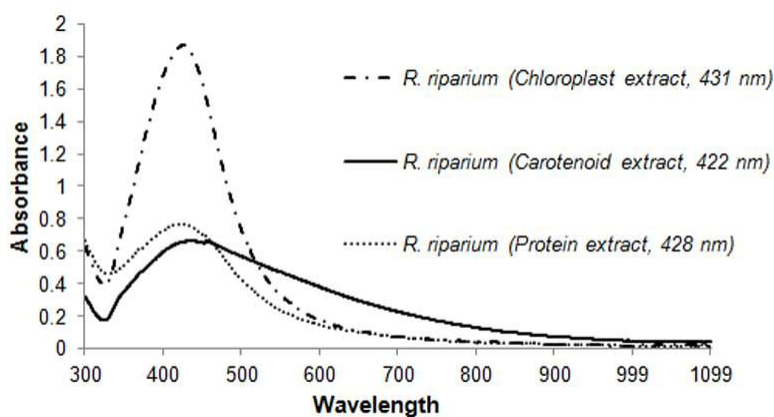


**Fig 5** Uv-vis spectra of the SNP synthesized by extracted protein, chloroplast and carotenoids of *Rhizoclonium*.

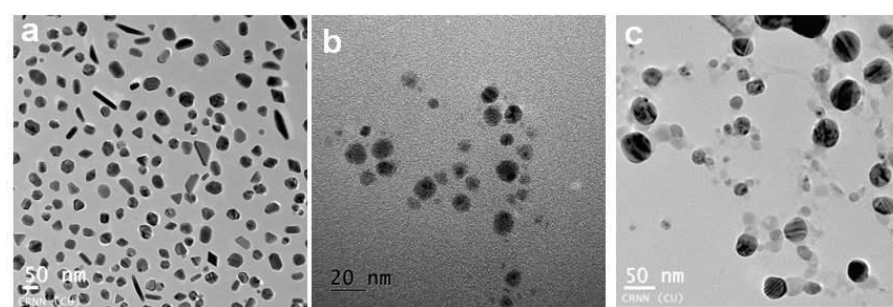


**Fig 6** TEM images of SNP synthesized by carotenoids (a), protein (b) and chloroplast (c).

Agarose gel electrophoresis of DNA-SNP revealed that in maximum SNP concentration no DNA band was observed in lane 2 (SNP concentration  $0.5\text{mg ml}^{-1}$ ). A competitive binding of nanoparticles with ethidium bromide was observed in agarose gel electrophoresis. Non-availability of binding site for ethidium bromide revealed that intercalation process did not occur (MubarakAli et al. 2014). The presence of functional groups (-CH) on the particle surfaces confirmed by FTIR study can help to bind with DNA. Further, the electrostatic

interaction between particle and DNA increase the binding affinity. The synthesized particles were less negatively charged, since they were suspended in water. The data taken together confirmed the interactions between unmodified SNP particles and DNA molecules. Here we observed a very good DNA binding affinity of the SNP particles without any surface modification.

After exposure in SNP, cell wall of *Chlorococcum* turned brown in color and confirmed that SNP can easily enter within the algal cells by diffusion. Then it changes the structure of cell membrane and causes the cell death. SNP is also able to release free radicals and these free radicals are able to break the cell membrane and make it porous which finally lead to cell death (Sondi and Salopek-Sondi, 2004).

Initial increase and overall decrease of protein and carbohydrate content in silver exposure indicated metal stress response of green algae. The decrease of chlorophyll content indicated cellular toxicity. Inhibition of photosynthetic pigment biosynthesis is one of the primary events in plants during heavy metal stress (Cenkci et al. 2010). Upregulation of stress enzymes such as catalase, SOD, and APX together with carotenoid content indicated active protection against  $Ag^+$  stress. Carotenoids serve as antioxidants against free radicals and photochemical damage (Sengar et al. 2008), therefore it is more active against oxidative stress.

Carotenoids played a major role in SNP synthesis because of their electron donating ability. Sliwka et al. (2007) reported that hydrophilic condition enhances the electron transfer ability of carotenoids. In our study, the entire experiment was done in water-based medium which also helped in transferring electron to  $Ag^+$ . The cell-free proteins extracted from *Rhizoclonium* reduced  $Ag^+$  ions at 4°C which confirmed that most of the enzymes lost their reducing ability at high temperature. Das et al. 2012 reported that the carboxyl and amine groups of phosphoproteins are accountable for  $Ag^+$  reduction. The pigment bearing extracted chloroplast transferred electrons to  $Ag^+$  from the photosynthetic electron transport chain (Zhang et al. 2011; Shabnam and Pardha-Saradhi 2013). A direct role of photosynthetic electron transport chain in reduction of metal ions and synthesis of NP was reported by Shabnam and Pardha-Saradhi (2013).

In conclusion, it can be said that synthesis of SNP by algal filament is dependent on various cellular components like carotenoids, protein and chloroplast. These fractionated cellular components of *R. riparium* have been identified as metal ion reducing agents. The SNP showed effective algicidal activity against green alga, *Chlorococcum infusionum*. These particles also showed its efficiency in binding with DNA and this DNA-SNP conjugate has potential application in the field of medical science.

#### Acknowledgements

Authors would like to thank Urmila Goswami, Sujoy Debnath, Tridib Das, Soumitra Paul and Prasun Mukherjee for their immense help during this research work.

#### References

- Ahmad, A. Mukherjee, P. Senapati, S. Mandal, D. Khan, M.I. Kumar, R. Sastry, M. 2003 Extracellular biosynthesis of silver nanoparticles using the fungus *Fusarium oxysporum*. *Colloids. Surf. B.* **28** : 313–318
- Annon, D.I. 1949 Copper enzymes in isolated chloroplasts, polyphenoxides in *Beta vulgaris*. *Plant. Physiol.* **24** : 1–15
- Beauchamp, C.O. Fridovich, I. 1971 Superoxide dismutase. Improved assays and an assay applicable to acrylamide gels. *Anal. Biochem.* **44** : 276–287
- Cenkci, S. Cigerci, I.H. Yildiz, M. Özay, C. Bozdogan, A. Terzi, H. 2010 Lead contamination reduces chlorophyll biosynthesis and genomic template stability in *Brassica rapa* L. *Environ. Exp. Bot.* **67** : 467–73
- Daniel, M.C. Astruc, D. 2004 Gold nanoparticles: assembly, supramolecular chemistry, quantum-size-related properties, and applications toward biology, catalysis, and nanotechnology. *Chem. Rev.* **104** : 293– 346.
- Das, S.K. Dickinson, C. Lafir, F. Brougham, D.F. Marsili, E. 2012 Synthesis, characterization and catalytic activity of gold nanoparticles biosynthesized with *Rhizopus oryzae* protein extract. *Green. Chem.* **14** : 1322–1334
- Doyle, J.J. Doyle, J.L. 1990 Isolation of plant DNA from fresh tissue. *Focus.* **12** : 13–15
- Famarzi, M.A. Forootanfar, H. 2011 Biosynthesis and characterization of gold nanoparticles produced by laccase from *Paraconiothyrium variable*. *Colloids. Surf. B.* **87** : 23–27

Fen, L.B. Chen, S. Kyo, Y. Herpoldt, K.L. Terrill, N.J. Dunlop, I.E. Mcphail, D.S. Shaffer, M.S. Schwander, S.

Gow, A. Zhang, J. Chung, K.F. Tetley, T.D. Porter, A.E. Ryan, M.P. 2013 The stability of silver nanoparticles in a model of pulmonary surfactant. *Environ. Sci. Technol.* **47** : 11232–11240

Gajbhiye, M. Kesharwani, J. Ingle, A. Gade, A. Rai, M. 2009 Fungus mediated synthesis of silver nanoparticles and their activity against pathogenic fungi in combination with fluconazole. *Nanomed. Nanotechnol. Biol. Med.* **5** : 382–386

Ganesh Babu, M.M. Gunasekaran, P. (2009) Production and structural characterization of crystalline silver nanoparticles from *Bacillus cereus* isolate. *Colloids. Surf. B.* **74** : 191–195

Gole, A. Dash, C. Ramakrishnan, V. Sainkar, S. Mandale, A. Rao, M. Sastry, M. 2001 Pepsin-gold colloid conjugates: preparation, characterization, and enzymatic activity. *Langmuir.* **17** : 1674–1679

Gurunathan, S. Kalishwaralal, K. Vaidyanathan, R. Venkataraman, D. Pandian, S.R.K. Muniyandi, J. Hariharan, N. Eom, S.H. 2009 Biosynthesis purification and characterization of silver nanoparticles using *Escherichia coli*. *Colloids. Surf. B.* **74** : 328–335

Hodge, J.E. Hodge, B.T. 1962 Carbohydrate chemistry. Academic Press, New York

Huang, J. Li, Q. Sun, D. Lu, Y. Su, Y. Yang, X. 2007 Biosynthesis of silver and gold nanoparticles by novel sundried *Cinnamomum camphora* leaf. *Nanotechnology.* **18** : 105104

Huang, T. Nallathamby, P.D. Xu, X.N. 2008 Photostable Single-Molecule Nanoparticle Optical Biosensors for Real-Time Sensing of Single Cytokine Molecules and Their Binding Reactions. *J. Am. Chem. Soc.* **130** : 17095–17105

Ingle, A.P. Gade, A.K. Pierrat, S. Sønnichsen, C. Rai, M.K. 2008 Mycosynthesis of silver nanoparticles using the fungus *Fusarium acuminatum* and its activity against some human pathogenic bacteria. *Curr. Nanosci.* **4** : 141–144

Ip, M. Lui, S.L. Poon, V.K.M. Lung, I. Burd, A. 2006 Antimicrobial activities of silver dressings: An in vitro comparison. *Int. J. Med. Microbiol.* **55** : 59-63

Jena, J. Pradhan, N. Dash, B.P. Panda, P.K. Mishra, B.K. 2014 Pigment mediated biogenic synthesis of silver nanoparticles using diatom *Amphora* sp. and its antimicrobial activity. *J. Saudi. Chem. Soc.* **19** : 661–666

Jeong, S.H. Yeo, S.Y. Yi, S.C. 2005 The effect of filler particle size on the antibacterial properties of compounded polymer/silver fibers. *J. Mater. Sci.* **40** : 5407- 5411

Kalishwaralal, K. Deepak, V. Pandian, S.R.K. Kottaisamy, M. BarathManiKanth, S. Kartikeyan, B. Gurunathan, S. 2010 Biosynthesis of silver and gold nanoparticles using *Brevibacterium casei*. *Colloids. Surf. B.* **77** : 257–262

Kleinegris, D.M.M. Es, M.A. Janssen, M. Brandenburg, W.A. Wijffels, R.H. 2010 Carotenoid fluorescence in *Dunaliella salina*. *J. Appl. Phycol.* **22** : 645–649

Kunst, L. Browse, J. Somerville, C. 1988 Altered regulation of lipid biosynthesis in a mutant of *Arabidopsis* deficient in chloroplast glycerol-3-phosphate acyltransferase activity. *Proc. Natl. Acad. Sci.* **85** : 4143-47

Lara, H.H. Ayala-Nunez, N.V. Turrent, L.I. Rodriguez-Padilla, C. 2010 Mode of antiviral action of silver nanoparticles against HIV1. *J. Nanobiotechnol.* **8** : 1-10

Lee, S. Cha, E.J. Park, K. Lee, S.Y. Hong, J.K. Sun, I.C. Kim, S. Choi, K. Kwon, I.C. Kim, K. Ahn, C.H. 2008 A Near-Infrared-Fluorescence-Quenched Gold-Nanoparticle Imaging Probe for In Vivo Drug Screening and

Protease Activity Determination. *Angewandte. Chemie.* **120** : 2846–2849

Lengke, F.M. Fleet, E.M. Southam, G. 2007 Biosynthesis of silver nanoparticles by filamentous cyanobacteria a from a silver (I) nitrate complex. *Langmuir.* **23**:2694- 2699

Liu, Y. Huang, C.Z. 2012 One-step conjugation chemistry of DNA with highly scattered silver nanoparticles for sandwich detection of DNA. *Analyst.* **137** : 3434–3436

Lowrey, O.H. Rosenbrough, N.J. Farr, A.L. Randall, R.J. 1951 Protein measurement with the folin phenol reagent. *J. Biol. Chem.* **193** : 265–327

Lu, J. Moon, K.S. Xu, J. Wong, C.P. 2006 Synthesis and dielectric properties of novel high-K polymer composites containing in-situ formed silver nanoparticles for embedded capacitor applications. *J. Mater. Chem.* **16** : 1543–1548

Marambio-Jones, C. Hoek, E.M.V. 2010 A review of the antibacterial effects of silver nano materials and potential implications for human health and the environment. *J. Nanopart. Res.* **12** : 1531-1551

MubarakAli, D. HarishNag, K. SheikSyedIshack, K.A. Baldev, E. Pandiaraj, D. Thajuddin, N. 2013 Gold nanoparticles from pro and eukaryotic photosynthetic microorganisms—comparative studies on synthesis and its application on biolabelling. *Colloids. Surf. B.* **103** : 166–173

MubarakAli, D. Thajuddin, N. Jeganathan, K. Gunasekaran, M. 2011 Plant extract mediated synthesis of silver and gold nanoparticles and its antibacterial activity against clinically isolated pathogens. *Colloids. Surf. B.* **85** : 360–365

Mukherjee, P. Ahmad, A. Mandal, D. Senapati, S. Sainkar, S.R. Khan, M.I. Parishcha, R. Ajaykumar, P.V. Alam, M. Kumar, R. Sastry, M. 2001 Fungus-mediated synthesis of silver nanoparticles and their immobilization in the mycelial matrix: a novel biological approach to nanoparticle synthesis. *Nano. Lett.* **1** : 515–519

Nakano, Y. Asada, K. 1981 Hydrogen peroxide is scavenged by ascorbate specific peroxidase in spinach chloroplasts. *Plant. Cell. Physiol.* **22** : 867–880

Nanda, A. Saravanan, M. 2009 Biosynthesis of silver nanoparticles from *Staphylococcus aureus* and its antimicrobial activity against MRSA and MRSE. *Nanomedicine.* **5** : 452–456

Parial, D. Pal, R. 2015 Biosynthesis of monodispersed gold nanoparticles by green alga *Rhizoclonium fontinale* and associated biochemical change. *J. Appl. Phycol.* **27** : 975–984

Pradeep, T. and Anshup 2009 Noble metal nanoparticles for water purification: A critical review. *Thin. Solid. Films.* **517** : 6441–6478

Pugazhenthiran, N. Anandan, S. Kathiravan, G. Prakash, N.K.U. Crawford, S. Ashokkumar, M. 2009 Microbial synthesis of silver nanoparticles by *Bacillus* sp. *J. Nanopart. Res.* **11** : 1811–1815

Rajasekharreddy, P. Rani, P.U. Sreedhar, B. 2010 Qualitative assessment of silver and gold nanoparticle synthesis in various plants: a photobiological approach. *J. Nanoparticle. Res.* **12** : 1711–1721

Roychoudhury, P. Pal, R. 2014 Synthesis and characterization of nanosilver—a blue green approach. *Ind. J. Appl. Res.* **4** : 54–56

Roychoudhury, P. Bhattacharya, A. Dasgupta, A. Pal, R. 2016 Biogenic synthesis of gold nanoparticle using fractionated cellular components from eukaryotic algae and cyanobacteria. *Phycol. Res.* doi: 10.1111/pre.12127.

Sadashivam, S. Manickam, A. 1996 Biochemical methods, New Age International Pvt Ltd, New Delhi

- Samadi, N. Golkaran, D. Eslamifar, A. Jamalifar, H. Fazeli, M.R. Mohseni, F.A. 2009 Intra/extracellular biosynthesis of silver nanoparticles by an autochthonous strain of *Proteus mirabilis* isolated from photographic waste. *J. Biomed. Nanotechnol.* **5** : 247–253
- Sengar, R.S. Gupta, S. Gautam, M. Sharma, A. Sengar, K. 2008 Occurrence uptake accumulation and physiological responses of nickel in plants and its effects on environment. *Res. J. Phytochem.* **2** : 44–60
- Shabnam, N. Pardha-Saradhi, P. 2013 Photosynthetic electron transport system promotes synthesis of Au-nanoparticles. *PLoS. One.* **8** : 71123
- Shaligram, N.S. Bule, M. Bhambure, R. Singhal, R.S. Singh, S.K. Szakacs, G. Pandey, A. 2009 Biosynthesis of silver nanoparticles using aqueous extract from the compactin producing fungal strain. *Process. Biochem.* **44** : 939–943
- Shankar, S.S. Rai, A. Ahmad, A. Sastry, M. 2004 Rapid synthesis of Au, Ag and bimetallic Au core–Ag shell nanoparticles using Neem (*Azadirachta indica*) leaf broth. *J. Colloid. Interface. Sci.* **275** : 496–502
- Sintubin, L. Windt, W.D. Dick, J. Mast, J. Ha, D.V. Verstraete, W. Boon, N. 2009 Lactic acid bacteria as reducing and capping agent for the fast and efficient production of silver nanoparticles. *Appl. Microbiol. Biotechnol.* **84** : 741–749
- Sliwka, H.R. Melø, T.B. Foss, B.J. 2007 Electron- and energy-transfer properties of hydrophilic carotenoids. *Chem. Eur. J.* **13** : 4458–66
- Sondi, I. Salopek-Sondi, B. 2004 Silver nanoparticles as antimicrobial agent: a case study on *E coli* as a model for Gram-negative bacteria. *J. Colloid. Interface. Sci.* **275** : 177–182
- Verma, V.C. Kharwar, R.N. Gange, A.C. 2010 Biosynthesis of antimicrobial silver nanoparticles by the endophytic fungus *Aspergillus clavatus*. *Nanomedicine.* **5** : 33–40
- Zhang, Y.X. Zheng, J. Gao, G. Kong, Y.F. Zhi, X. Wang, K. Zhang, X.Q. Cui, X.D. 2011 Biosynthesis of gold nanoparticles using chloroplasts. *Int. J. Nanomedicine.* **6** : 2899–906